

RESSALVA

Atendendo solicitação do(a)
autor(a), o texto completo desta tese
será disponibilizado somente a partir
de 13/11/2019.

PROGRAMA DE PÓS-GRADUAÇÃO EM CIÊNCIA DOS MATERIAIS

“Study on sugar cane straw ash (SCSA) in alkali-activated binders”

JOÃO CLÁUDIO BASSAN DE MORAES

Ilha Solteira
2017

PROGRAMA DE PÓS-GRADUAÇÃO EM CIÊNCIA DOS MATERIAIS

“Study on sugar cane straw ash (SCSA) in alkali-activated binders”

JOÃO CLÁUDIO BASSAN DE MORAES

Supervisor: Prof. Dr. Jorge Luís Akasaki
Co-Supervisor: Prof. Dr. Jordi Payá Bernabeu

A thesis submitted to the Faculdade de Engenharia – Campus de Ilha Solteira/UNESP, for the degree of Doctor in Materials Science and Engineering.

Area of knowledge: Materials Science and Engineering.

Ilha Solteira
2017

FICHA CATALOGRÁFICA

Desenvolvido pelo Serviço Técnico de Biblioteca e Documentação

M827s Moraes, João Claudio Bassan de.
Study on sugar cane straw ash (SCSA) in alkali-activated binders / João Claudio Bassan de Moraes. -- Ilha Solteira: [s.n.], 2017
187 f. : il.

Tese (doutorado) - Universidade Estadual Paulista. Faculdade de Engenharia de Ilha Solteira. Área de conhecimento: Ciência e Engenharia de Materiais, 2017

Orientador: Jorge Luís Akasaki
Co-orientador: Jorge Juan Payá Bernabeu
Inclui bibliografia

1. Alternative material. 2. Sustainable material. 3. Compressive strength. 4. Microstructural studies.

CERTIFICADO DE APROVAÇÃO

TÍTULO DA TESE: Study on sugar cane straw ash (SCSA) in alkali-activated binders

AUTOR: JOÃO CLAUDIO BASSAN DE MORAES

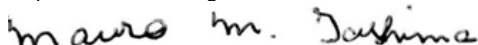
ORIENTADOR: JORGE LUIS AKASAKI

COORIENTADOR: JORGE JUÁN PAYÁ BERNABEU

Aprovado como parte das exigências para obtenção do Título de Doutor em CIÊNCIA DOS MATERIAIS, área: CIÊNCIA E ENGENHARIA DOS MATERIAIS pela Comissão Examinadora:



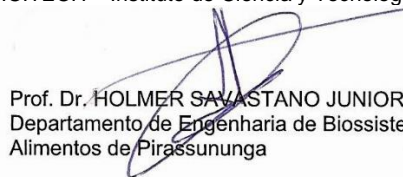
Prof. Dr. JORGE LUIS AKASAKI
Departamento de Engenharia Civil / Faculdade de Engenharia de Ilha Solteira



Prof. Dr. MAURO MITSUUCHI TASHIMA
Departamento de Engenharia Civil / Faculdade de Engenharia de Ilha Solteira



Profa. Dra. MARIA VICTORIA BORRACHERO ROSADO
ICITECH – Instituto de Ciencia y Tecnología del Hormigón / Universitat Politècnica de Valencia



Prof. Dr. HOLMER SAVASTANO JUNIOR
Departamento de Engenharia de Biossistemas / Faculdade de Zootecnia e Engenharia de Alimentos de Pirassununga



Prof. Dr. EMÍLIO CÉSAR CAVALCANTE MELO DA SILVA
CENPES – Centro de Pesquisa da Petrobras / Petróleo Brasileiro

Ilha Solteira, 13 de novembro de 2017



UNIVERSIDADE ESTADUAL PAULISTA
"JÚLIO DE MESQUITA FILHO"

I dedicate this thesis to my
parents, Cássia Regina and
João Batista, and my sister,
Maria Júlia.

ACKNOWLEDGMENTS

I would like to thank my mother Cássia Regina, my father João Batista, my sister Maria Júlia, my aunt Claudia and Meggy to the support and love.

I would like to thank the supervisors and friends, Jorge Akasaki and Jordi Payá, for the knowledge and the opportunity.

I would like to thank the professor and friend Mauro Tashima for helping me in my scientific career and for sharing funny moments.

I would like to thank the professors and friends, José Luiz Melges, María Victoria Borrachero and José Monzó, for the support and knowledge to write the thesis. Thanks also to professor João Carlos Moraes for supporting the qualifying exam. Thanks to professors José Lollo, Rogério Rodrigues, Renato Bertolino, Tsunao and Haroldo Bernardes from Civil Engineering Department for the knowledge provided in my professional career.

I would like to thank my friends from the Civil Engineering Graduate, Priscila, Heitor, Franciéli and Jônatas for the support and funny moments.

I would like to thank all my friends from GIQUIMA, specially to Lourdes and Alba for the strong friendship and for making my year in Valencia very especial. Thanks also to Lucía, Ariel, Patrícia, Jesús, Amin, Yasna, Noelia, Clara, Edwin, Ricardo, Álvaro, Fausto and Manolo "Mister" Paredes. In addition, I would like to thank the researchers and workers from ICITECH for my great year in Valencia.

I would like to thank all my friends from MAC group, João Victor, Adriana, Alex, Danilo, Alan and Thiago Trentin, for the funny and professional moments.

I would like to thank the best neighborhood I ever had in Ilha Solteira: Bruna, Fernanda, Gabriel and Paula.

I would like to thank my friends from Marília, Everton, Bia, Bruno and Renata, for the funny moments.

I would like to thank my friends from Ilha Solteira for the supporting and taking care of me: Estéfani, folks from Equilibrium gym, Mariana Lopes and family, Fernando Tangerino and Angelo Doimo.

I would like to thank my friends from Valencia for one of the best trips I have ever gone: Luigi, Jana, Francesco, Theresa, Lech and Iona.

I would like to thank my virtual friends, but they were closer than ever: Kelly, Gisele and the FC Barcelona group (Caio, Fabielle, Edvande, Drielle, Filipe, Poly and Laiza).

I would like to thank the folks who work in the Civil Engineering Department: Sandra, José Carlos, Juliana, Gilson, Flavio, Ozias, Ademir and Marcelo.

I would like to thank Jaira and Maria Gercy for taking care of me during these years.

I would like to thank CNPq and CAPES for the scholarship.

Finally, thanks to everyone who contributed directly or indirectly to this thesis.

RESUMO

Aglomerantes ativados alcalinamente (AAA) são obtidos da combinação de um precursor sólido (geralmente um aluminossilicato) e uma solução alcalina de alta concentração. As vantagens de utilizar este novo tipo de aglomerante comparado ao cimento Portland, um aglomerante convencional, são as menores emissões de CO₂, menor consumo de energia e a possibilidade de utilizar matérias prima renováveis e/ou resíduos. Neste sentido, este trabalho apresenta um novo resíduo da indústria da cana de açúcar: a folha de cana de açúcar. A folha apresenta um poder calorífico interessante; portanto, ela pode ser utilizada como biomassa para produzir energia através um processo de queima. Depois deste procedimento, é gerado um novo resíduo: a cinza de folha de cana de açúcar (CF). Esta cinza não apresenta uma destinação correta, então este trabalho tem como intenção utilizar esta cinza como material prima em AAA. A CF foi avaliada de duas formas: como precursor sólido e como matéria prima para produzir a solução alcalina. No primeiro modo, a CF foi utilizada em sistemas combinados com a escória de alto forno (EAF) ativado com ambas soluções de NaOH e NaOH/silicato de sódio. No segundo modo, a CF foi utilizada como fonte de sílica para produzir a solução alcalina com o NaOH em AAA baseados em EAF. Os sistemas foram estudados através da resistência a compressão de argamassas e pelo estudo da microestrutura de pastas. Ensaio realizados para avaliar a microestrutura foram a difração de raios-X (DRX), espectroscopia de infravermelho por transformada de Fourier (EITF), análise termogravimétrica (ATG), microscopia eletrônica de varredura (MEV) e porosimetria por intrusão de mercúrio (PIM). Resultados dos ensaios mostraram que a CF melhorou as propriedades mecânicas dos AAA baseados em EAF nos dois modos, como precursor sólido e como fonte de silício para a solução ativadora. Estes resultados permitem concluir que a CF pode ser utilizada em AAA, dando uma destinação ao resíduo.

Palavras chave: Material alternativo. Material sustentável. Resistência à compressão. Estudos microestruturais.

ABSTRACT

Alkali-activated binders (AAB) are obtained from a combination of a solid precursor (generally an aluminosilicate) and a high concentrated alkaline solution. The advantages of using this new type of binder compared to the Portland cement, a conventional binder, are the less CO₂ emissions, lower energy consumption and the possibility of using renewable and/or residues as raw materials. In this way, this work presents a new residue from the sugar cane industry: the sugar cane straw. The straw presents an interesting calorific value; therefore, it can be utilised as biomass to produce energy by a burning process. After this procedure, it is generated another waste: the sugar cane straw ash (SCSA). This ash does not have an appropriate destination, then this work intends to utilise this ash as raw material in AAB. SCSA was evaluated in both ways: as solid precursor and as raw material to produce the alkaline solution. In the first way, SCSA was utilised in combined systems with blast furnace slag BFS activated with both NaOH and NaOH/sodium silicate solutions. In the second one, the SCSA was utilised as silica source to produce the alkaline solution with NaOH in BFS-based systems. These systems were assessed by the compressive strength of mortars and by microstructural studies on pastes. Tests carried out to assesses their microstructure were X-ray diffraction (XRD), Fourier transform infrared spectroscopy (FTIR), thermogravimetric analysis (TGA), field emission scanning electron microscopy (FESEM), and mercury intrusion porosimetry (MIP). Results of the tests showed that the SCSA improved the mechanical properties of BFS-based AAB in both methods, as solid precursor and as silica source to produce the activating solution. These results allow to conclude that the SCSA can be utilised in AAB, giving it a suitable destination.

Keywords: Alternative material. Sustainable material. Compressive strength. Microstructural studies.

FIGURES LIST

Figure 1.1	Experimental program of the present doctoral thesis	18
Figure 2.1	Scheme of types of binders related to the Ca, Al and M ⁺ content, emphasizing the classification of alkali-activated binders and geopolymers (PROVIS, 2014)	20
Figure 2.2	Development in the accumulated publications number in Scopus/Elsevier database of the words "alkali-activated binders" (dotted line) and "geopolymer" (solid line) presented in title, abstract or keywords (PACHECO-TORGAL et al., 2015)	21
Figure 2.3	Proposed model to formation of BFS-based alkali-activated binders: a) role from the alkalis in the reaction (being R ⁺ the alkaline cation), and b) gel formation (GARCIA-LODEIRO et al., 2015)	23
Figure 2.4	A general view from the N-A-S-H gels produced in the alkaline activation of binders with low Ca-content (GARCIA-LODEIRO et al., 2015)	24
Figure 2.5	Reaction mechanism from the first step named destruction-coagulation: a) dissolution of Si-O-Si bonds, and b) dissolution of Si-O-Al bonds (GARCIA-LODEIRO et al., 2015)	25
Figure 2.6	Reaction mechanism from the second step named coagulation-condensation (GARCIA-LODEIRO et al., 2015)	26
Figure 2.7	Illustration of the gel formation in alkali-activated binders with low Ca-content (GARCIA-LODEIRO et al., 2015)	27
Figure 2.8	Studies on influence of sodium silicate in the compressive strength of BFS-based AAB: a) phosphorous BFS; and b) Acid, neutral and basic BFS (SHI et al., 2006)	29
Figure 2.9	Compressive strength results of combined systems composed by blast furnace slag and red clay brick waste (RCBW/BFS) after 28 days of curing at room temperature (RAKHIMOVA and RAKHIMOV, 2015)	30
Figure 2.10	Compressive strength results of binary systems composed by metakaolin and fly ash (MK/FA) after 7 and 28 days of curing at room temperature (ZHANG et al., 2014)	33
Figure 2.11	Compressive strength evolution of FA/POFA specimens studied in high temperatures (adapted from RANJBAR et al., 2014)	35
Figure 2.12	Comparison between CO ₂ footprints of concretes based on alkali-activated binders and OPC, highlighting the emissions from the alkaline activator (adapted from Turner; Collins, 2013)	37
Figure 2.13	Compressive strength versus reflux time of FCC-based alkali activated binders prepared with different siliceous sources combined with NaOH solutions: G-RHA (ground rice husk ash), O-RHA (original rice husk ash), quartz, control (commercial waterglass solution). Key: full line for compressive strength and dotted line for flexural strength (Bouzón et al., 2014)	38
Figure 2.14	Compressive strength of concrete manufactured with fly ash and palm oil fuel ash (BA geopolymer concrete) compared to one of Portland cement after sulfuric acid attack (ARIFFIN et al., 2013)	39

Figure 2.15	Compressive strength after temperature treatment of OPC mixtures and alkali-activated binders of solid precursors with a) high Ca content and b) low Ca content (TURKER et al., 2016; DUAN et al., 2015)	41
Figure 2.16	Mechanized harvesting of the sugar cane (UNICA, 2016)	42
Figure 2.17	Electrical conductivity of hydrated lime/RHA and hydrated lime/SCSA suspensions (VILLAR-COCINA, 2002)	43
Figure 2.18	Compressive strength of mortars cured after 60 days (GUZMÁN et al., 2011)	44
Figure 3.1	Loss of electrical conductivity (Lc) of suspensions studied at (a) 60 °C; (b) 50 °C; (c) 40 °C; and (d) 30 °C	62
Figure 3.2	pH variation (Δ pH) of the CH/SCSA suspensions at each temperature studied	63
Figure 3.3	DTG curves of the solid part of the suspensions after electrical conductivity measurements at 40 °C.	64
Figure 3.4	FTIR spectra of 3:7 and 5:5 CH/SCSA pastes after 1, 3, 7, and 28 days of curing at 40 °C	66
Figure 3.5	DTG curves of 5:5 and 3:7 CH/SCSA pastes from 1 to 28 days of curing at 40 °C	68
Figure 3.6	SEM images of 3:7 CH/SCSA paste after 28 days of curing cured at 40 °C	70
Figure 4.1	X-Ray Diffraction of SCSA	76
Figure 4.2	SEM images of SCSA	77
Figure 4.3	Compressive strength of Portland cement mortars	80
Figure 4.4	Compressive strength of alkaline activated mortars	81
Figure 5.1	Calculated γ factor for specimens with BFS/SCSA ratios of 85/15, 75/25, 67/33 and 50/50, in the ϵ value range of 0-0.75, after: a) 3 days of curing, b) 7 days of curing, c) 28 days of curing and d) 90 days of curing (at 25°C)	91
Figure 5.2	DTG curves for the N-100/0 (a), SS50-100/0 (b), N-75/25 (c), SS50-75/25 (d), N-50/50 (e) and SS50-50/50 (f) pastes cured for 7, 28 and 90 days at 25°C	92
Figure 5.3	FTIR spectra for the N-100/0 (a), SS50-100/0 (b), N-75/25 (c), SS50-75/25 (d), N-50/50 (e) and SS50-S50 (f) pastes cured for 7, 28 and 90 days at 25°C	94
Figure 5.4	XRD patterns for the raw materials, BFS and SCSA, and for the N-100/0 and N-50/50 pastes, cured for 28 days at 25°C. (Keys: Q: Quartz; C: Calcite; W: Wollastonite; N: Termonatrite; T: Hydrotalcite; K: Katoite; S: Stratlingite; H: Hydrosodalite; P: Hydrated Nepheline)	95
Figure 5.5	FESEM images of N-100/0 (a and b) and N-50/50 (c and d) after 28 days of curing at 25°C.	96
Figure 6.1	Values of the ϕ ratio for mortars containing SCSA at 7, 28 and 90 days of curing	112

Figure 6.2	XRD patterns of the raw materials (BFS and SCSA) and the pastes 28-0-100/0, 28-0-75/25, 28-0.75-100/0 and 28-0.75-75/25 after 90 days of curing (Key: Q: quartz; C: calcite, H: hydrotalcite; K, katoite; C-S-H: calcium silicate hydrate)	113
Figure 6.3	FTIR spectra of the raw materials (BFS and SCSA) and the pastes 28-0-100/0, 28-0-75/25, 28-0.75-100/0 and 28-0.75-75/25 after 7, 28 and 90 days of curing	114
Figure 6.4	DTG curves of the pastes 28-0-100/0, 28-0-75/25, 28-0.75-100/0 and 28-0.75-75/25 after 7, 28 and 90 days of curing	117
Figure 6.5	Relationships between thermogravimetric mass losses for pastes (P_g , 35-250°C; and P_t , 35-1000°C) and the compressive strength of mortars	118
Figure 6.6	MIP curves of the pastes 28-0-100/0, 28-0-75/25, 28-0.75-100/0 and 28-0.75-75/25 after 90 days of curing: a) differential, and b) accumulated distribution	119
Figure 6.7	FESEM micrographs of BFS activated paste with NaOH (28-0-100/0): a) general view of the paste with an unreacted BFS particle (spot A) and gel (spot B); b) detailed view of the gel; c) in-lens micrograph showing BFS unreacted particle (spot A) and main gel (spot B); d) enlarged zone from c), in which a denser gel is shown (spot C)	120
Figure 6.8	FESEM micrographs of BFS/SCSA activated paste with NaOH (28-0-75/25): a) general view of the paste; b) general view of formed gels (spot D shows a porous gel, and spot E, a compacted gel); c) detailed view of both gels; d) in-lens view (lighter area for porous gel, and darker are for compacted gel)	122
Figure 6.9	FESEM micrographs of BFS activated paste with NaOH and sodium silicate (28-0.75-100/0): a) general view of the paste with some gel formation (spot F shows a porous gel, and spot G, a compacted gel); b) detailed view of formed gels; c) detailed view of sheet-like crystals (spot H, stratlingite); d) pirssonite crystals surrounded by gels	123
Figure 6.10	FESEM micrographs of BFS/SCSA activated paste with NaOH and sodium silicate (28-0.75-75/25): a) general view of the paste with some gel formation (spot J) and a quartz particle (spot K); b) detailed view of compacted gel; c) detailed view of gel; d) pirssonite crystals surrounded by gels.	124
Figure 7.1	Influence of the H_2O/Na_2O ratio by line adjustment on BFS/SCSA proportions of 100/0 (a), 90/10 (b), 80/20 (c) and 70/30 (d) after 3, 7, 28 and 90 days of curing at 25 °C	137
Figure 7.2	σ_{SCSA} factor for SCSA percentage replacements of 10, 20 and 30% after: a) 3; b) 7; c) 28; and d) 90 days of curing at 25 °C	140
Figure 7.3	Best BFS/SCSA proportion for the H_2O/Na_2O ratios of: a) 11.1; b) 13.9; and c) 18.5 after 3, 7, 28 and 90 days of curing at 25 °C	141

Figure 7.4	Non-linear fitting surface of compressive strength values considering all the results after 90 days of curing. Points linked by a solid curve represent the optimum percentage of SCSA in the mixture.	142
Figure 7.5	X-ray diffraction patterns of the raw material and pastes after 90 days of curing: a) BFS and SCSA (raw materials), 19-100/00 and 19-80/20 (pastes); b) BFS and SCSA (raw materials), 19-80/20, 14-80/20 and 11-80/20 (pastes). Key: Q: quartz; C-S-H: semi-crystalline C-S-H; H: hydrotalcite; K: katoite; F: faujasite; C: calcite; S: hydrosodalite	144
Figure 7.6	FTIR spectra of the raw materials (BFS and SCSA) and pastes cured for: a and d) 7 days; b and e) 28 days; and c and f) 90 days at 25 °C. Study on the effect of SCSA content (see a, b and c graphs). Study on the effect of the sodium hydroxide concentration (see d, e and f graphs)	146
Figure 7.7	DTG curves of the pastes: 19-100/0, 19-90/10, 19-80/20 and 19-70/30 cured after a) 7 days, b) 28 days and c) 90 days; and 19-80/20, 14-80/20 and 11-80/20 cured after d) 7 days, e) 28 days and f) 90 days.	149
Figure 7.8	FESEM micrographs of the pastes: a) 19-100/0; and b) 19-80/20 cured after 90 days	151
Figure 7.9	FESEM micrographs of the pastes: a) 19-80/20; b) 14-80/20; and c) 11-80/20 cured after 90 days	152
Figure 8.1	Temperature evolution with time in the dissolution of sodium hydroxide (32.4 g) in water (202.5 g) inside the thermal bottle	165
Figure 8.2	Compressive strength values of mortars (cured at 65 °C for 3 days) with activator prepared by thermal bottle treatment in different reaction time (τ) of 0, 6, 24 and 48 hours	169
Figure 8.3	XRD patterns of raw materials (SCSA and BFS) and pastes (SCSA-1.46-24, SCSA-1.46-0, NH-0 and SS-1.46) cured after 3 days at 65 °C. Keys: Q: quartz; C: calcite; H: hydrotalcite; F: faujasite; C-S-H: calcium silicate hydrate; K: katoite.	171
Figure 8.4	FTIR spectra of raw materials (SCSA and BFS) and pastes (SCSA-1.46-24, SCSA-1.46-0, NH-0 and SS-1.46) cured after 3 days at 65 °C	172
Figure 8.5	DTG curves of pastes (SCSA-1.46-24, SCSA-1.46-0, NH-0 and SS-1.46) cured after 3 days at 65 °C (numbers close to main peaks are in °C)	173
Figure 8.6	FESEM micrographs of the paste SCSA-1.46-24	174
Figure 8.7	FESEM micrographs of the paste SCSA-1.46-0	175
Figure 8.8	Compressive strength values of mortars (cured at 65 °C for 3 days) with activator prepared by thermal bottle treatment in different SiO ₂ /Na ₂ O molar ratio (ϵ) of 0 (only NaOH), 0.73, 1.09, 1.46 and 1.82	176

Figure 8.9	FESEM micrographs of the paste NH-0	178
Figure 8.10	Comparison of compressive strength values of mortars (cured at 65 °C for 3 days and 20 °C for 28 days) obtained from SCSA, SS and RHA	179
Figure 8.11	FESEM micrographs of the paste SS-1.46	181

TABLES LIST

Table 3.1	Chemical composition of SCSA by percentage	60
Table 3.2	Mass loss related to the dehydration of pozzolanic reaction products (P_P) and calcium hydroxide (P_{CH}), and lime fixation of CH:SCSA pastes	68
Table 4.1	Chemical composition of blast furnace slag (BFS) and sugar cane straw ash (SCSA)	78
Table 5.1	Chemical composition of SCSA and BFS by weight percentage	87
Table 5.2	Specimens' names, compressive strength of mortars (MPa) and their standard deviations	91
Table 5.3	Mass losses for the N-100/0, N-75/25, N-50/50, SS50-100/0, SS50-75/25 and SS50-50/50) pastes cured for 7, 28 and 90 days at 25°C in defined temperatures ranges of TGA (35-180°C, 180-250°C and 250-600°C)	93
Table 6.1	Chemical characterisation of the solid precursors utilised in this paper (BFS and SCSA)	105
Table 6.2	Mixture dosage and specimen's names and tests carried out: compressive strength (R_c), X-ray diffraction (XRD), Fourier transform infrared spectroscopy (FTIR), Thermogravimetric analyses (TGA), Mercury intrusion porosimetry (MIP) and Field emission scanning electron microscopy (FESEM)	106
Table 6.3	Compressive strength of mortars (MPa) and their standard deviations	110
Table 6.4	Mass losses (%) for the pastes 28-0-100/0, 28-0-75/25, 28-0.75-100/0 and 28-0.75-75/25 after 7, 28 and 90 days of curing at different temperature ranges (35-250°C, 450-650°C, and total mass loss 35-1000°C)	117
Table 6.5	MIP results of the pastes 28-0-100/0, 28-0-75/25, 28-0.75-100/0 and 28-0.75-75/25 after 90 days of curing	119
Table 7.1	Chemical composition of the raw materials sugar cane straw ash (SCSA) and blast furnace slag (BFS) in weight percentages	134
Table 7.2	Specimen names, mixture designs (H_2O/Na_2O and BFS/SCSA ratios) and tests performed: compressive strength (R_c), X-ray diffraction (XRD), Fourier transform infrared spectroscopy (FTIR), thermogravimetric analysis (TGA) and field emission scanning electron microscopy (FESEM)	136
Table 7.3	Slope values from the graphic compressive strength versus H_2O/Na_2O ratio for the four BFS/SCSA proportions	138
Table 7.4	Mass losses from TGA curves in the 35–250 °C range ($P_{35-200^\circ C}$) and the total mass loss in 35–1000 °C range (P_T) in pastes cured for 7, 28 and 90 days at 25 °C	149
Table 8.1	Chemical composition of BFS, SCSA and RHA in wt%	164
Table 8.2	Mixtures and tests carried out	168
Table 8.3	Mass losses (%) of the pastes SCSA-1.46-24, SCSA-1.46-0, NaOH and SS-1.46 cured after 3 days at 65 °C in the test temperature intervals of 35-300 °C (P_{35-300}) and 300-1000 °C ($P_{300-1000}$)	173

TABLE OF CONTENTS

1	INTRODUCTION	16
1.1	OBJECTIVES	17
2.1	THESIS STRUCTURE	17
2	STATE OF THE ART	19
2.1	ALKALI-ACTIVATED BINDERS	19
2.1.1	Definition	19
2.1.2	History	20
2.1.3	Comparisons to the Portland cement	21
2.1.4	Alkali-activated binders reaction products	22
2.1.5	Solid precursor	27
2.1.6	Alkaline Activators	35
2.1.7	Durability	38
2.2	SUGAR CANE STRAW ASH	42
	REFERENCES	44
3	POZZOLANIC REACTIVITY STUDIES ON SUGAR CANE STRAW ASH	55
3.1	INTRODUCTION	56
3.2	MATERIALS AND METHODS	57
3.2.1	Materials	57
3.2.2	Equipment	58
3.3	RESULTS AND DISCUSSION	59
3.3.1	Sugar Cane Straw Ash Characterization	59
3.3.2	Electrical Conductivity Measurements	60
3.3.3	Fourier Transformed Infrared Spectroscopy	65
3.3.4	Thermogravimetric Analysis	66
3.3.5	Comparison of Results from Different Techniques	69
3.3.6	Scanning Electron Microscopy	69
3.4	CONCLUSIONS	70
	REFERENCES	71
4	PRELIMINARIES STUDIES ON SUGAR CANE STRAW ASH (SCSA) IN MORTARS OF PORTLAND CEMENT/SCSA AND BLAST-FURNACE SLAG/SCSA	74
4.1	INTRODUCTION	75
4.2	EXPERIMENTAL	76
4.2.1	Materials and Equipment	76
4.2.2	Experimental Procedures	78
4.2.2.1	<i>Portland cement mortars</i>	78
4.2.2.2	<i>Alkali-activated mortars</i>	78
4.3	RESULTS AND DISCUSSIONS	79
4.3.1	Compressive Strength of Portland Cement Mortars	79
4.3.2	Compressive Strength of Alkaline Activated mortars	80
4.3	CONCLUSIONS	81
	REFERENCES	81

5	SUGAR CANE STRAW ASH AS SOLID PRECURSOR IN ALKALI-ACTIVATED BINDERS BASED ON BLAST FURNACE SLAG: SOLUTIONS WITH [N+] OF 8 MOL.KG⁻¹ AND SiO₂/Na₂O RATIOS OF 0-0.75	84
5.1	INTRODUCTION	85
5.2	MATERIALS AND METHODS	86
5.2.1	Materials and Equipment	86
5.2.2	Alkali activated binder dosage	88
5.3	RESULTS AND DISCUSSION	88
5.4	CONCLUSIONS	96
	REFERENCES	97
6	SUGAR CANE STRAW ASH AS SOLID PRECURSOR IN ALKALI-ACTIVATED BINDERS BASED ON BLAST FURNACE SLAG: SOLUTIONS WITH [N+] OF 4 MOL.KG⁻¹ AND SiO₂/Na₂O RATIOS OF 0-0.75	100
6.1	INTRODUCTION	101
6.2	MATERIALS AND METHODS	104
6.2.1	Materials	104
6.2.2	Alkali activated binders' dosage and preparation	105
6.2.3	Test procedures for pastes and mortars	105
6.3	RESULTS AND DISCUSSION	107
6.3.1	Compressive strength of mortars	107
6.3.2	Microstructural studies	112
6.3	CONCLUSIONS	124
	REFERENCES	126
7	SUGAR CANE STRAW ASH AS SOLID PRECURSOR IN ALKALI-ACTIVATED BINDERS BASED ON BLAST FURNACE SLAG: SOLUTIONS WITH [N+] OF 6-10 MOL.KG⁻¹	129
7.1	INTRODUCTION	130
7.2	MATERIALS AND METHODS	133
7.2.1	Materials	133
7.2.2	Design of alkali-activated binders	134
7.2.3	Tests carried out for pastes and mortars	134
7.3	RESULTS AND DISCUSSION	137
7.3.1	Compressive strength of mortars	137
7.3.2	Microstructural studies	143
7.3.2.1	<i>X-ray diffraction (XRD)</i>	143
7.3.2.2	<i>Fourier transform infrared spectroscopy (FTIR)</i>	144
7.3.2.3	<i>Thermogravimetric analysis (TGA)</i>	147
7.3.2.4	<i>Field emission scanning electron microscopy (FESEM) and Energy-dispersive X-ray spectroscopy (EDS)</i>	150
7.4	CONCLUSIONS	152
8	SUGAR CANE STRAW ASH AS SILICA SOURCE TO PRODUCE THE ACTIVATING SOLUTION IN ALKALI-ACTIVATED BINDERS BASED ON BLAST FURNACE SLAG	160
8.1	INTRODUCTION	160
8.2	EXPERIMENTAL	162
8.2.1	Materials and Equipment	162

8.2.2	Alkali-activated materials preparation	164
8.2.3	Tests procedures	166
8.2.3	Alkali-activated materials studies	166
8.3	RESULTS AND DISCUSSION	168
8.3.1	Effect of the thermal bottle time (τ) for SCSA/NaOH suspensions (Section 1)	168
8.3.2	Effect of the SiO₂/Na₂O molar ratio (ϵ) for SCSA/NaOH suspensions (Section 2)	176
8.3.3	Comparison of SCSA to others silica sources (Section 3)	178
8.4	CONCLUSIONS	181
	REFERENCES	182
9	GENERAL CONCLUSIONS	185
10	PROPOSALS FOR FUTURE STUDIES	187

1 INTRODUCTION

Alkali-activated binders (AAB) are the new trend in the research of building construction materials. This type of material is obtained when a silico-aluminous material (also known as solid precursor) is combined with a high concentrated alkaline solution (activating solution) in appropriate proportions. The studies on this type of binder started in the last century with the purpose to reduce the Portland cement consumption. Authors highlighted some advantages of alkali-activated binders' mixtures when compared to the Portland cement: similar or higher compressive strength, improved durability and, mainly, less CO₂ emissions and energy consumption. However, these new kinds of binders present the disadvantages of handling difficult due the high alkalinity, and the several proportions and factors to analyse that influence the mechanical properties of the material (for example, the solid precursor and alkaline solution compositions).

Recent studies focused on the obtainment of new materials source (solid precursors and alkaline solution) for alkali-activated binders' production. The usual materials used as solids precursors are the blast-furnace slag, fly ash and metakaolin. About the alkaline sources in the preparation of the activating solution, hydroxides and silicates are the most common activators. New materials that are being researched in the preparation of alkali-activated binders are, in majority, residues from industry, agro-industry and building construction. This thesis presents a new agro-industry residue from sugar cane production in order to obtain an alkali-activated binder: the sugar cane straw ash (SCSA).

The issue of sugar cane starts in the increase of its production in the last years in Brazil due the production of alcohol and sugar: in only ten years (from 2004/2005 to 2014/2015), the increase was 64%. The state of Sao Paulo, where this research takes place, is the major sugar cane production in Brazil, which represents over than 50% of total production. Another important issue of the sugar cane is the harvesting process. Some years ago, the sugar cane harvesting used to be performed by a burning process in the cultivation area. However, an Agro-environmental protocol was signed to put an end on this burning procedure, making that the mechanized harvesting gains in importance on this scenario. In this type of harvesting, is generated a by-product that is composed by the dried and green leaves, which are mostly left on the cultivation field: the sugar cane straw. Due its interesting

calorific value, which is compared to the sugar cane bagasse, authors are studying new methods to collect and generate energy from this by-product. After this process to obtain energy from the straw, an ash is obtained: the sugar cane straw ash (SCSA). This residue does not present a suitable valorisation, and similar to other ashes from agro-industry (rice husk ash and sugar cane bagasse ash), it can be utilised in the building construction in alkali-activated binders.

9 GENERAL CONCLUSIONS

Sugar cane straw ash (SCSA) was successfully assessed as both solid precursor and silica source for the activating solution in alkali-activated binders based on blast furnace slag (BFS) with NaOH solutions.

SCSA obtained from an autocombustion process showed high reactivity since early curing times (see Chapters 3 and 4). Studies of thermogravimetric analysis (TGA) and Fourier transform infrared spectroscopy (FTIR) on pastes of SCSA and calcium hydroxide (CH) showed that the ash consumed all the CH in the first 3 days of curing at 40 °C. In the electrical conductivity tests, the SCSA was classified as medium reactivity (Chapter 3). Regarding to the use of the SCSA in mortars of Portland cement (as pozzolan) and blast-furnace slag (alkali-activated binders), the ash high reactivity was observed after 3 days of curing, where the SCSA-mortars presented similar or higher compressive strength.

As solid precursor in alkali-activated binders, SCSA partially replacing the BFS improved the alkali-activated mortars activated with NaOH for Na⁺ concentration of 4-10 mol.kg⁻¹ (see Chapters 5, 6 and 7). Compressive strength of SCSA-mortars activated with only NaOH reached higher values than the control with only blast-furnace slag/NaOH. In addition, the role of SCSA in the mixture was similar to the sodium silicate: SCSA mortars activated with only NaOH reached comparable compressive strength to a mortar with only BFS activated by both, sodium silicate and sodium hydroxide (see Chapters 5 and 6). Microstructural studies showed that the SCSA-containing mixtures presented a denser gel than one with only BFS and favoured the formation of zeolites. Therefore, the optimum use of SCSA in alkali-activated binders was replacing the BFS until 30% and using a Na⁺ concentration between 4-6 M

In the last part of the thesis, SCSA was successfully utilised as silica source in sodium solutions to produce a BFS-based alkali-activated binders (see Chapter 8). A certain amount of SCSA was mixed with NaOH in a thermal bottle during a determined time to produce the activating solution. The optimum dissolution time was 24 hours, and the optimum amount of SCSA, represented by the SiO₂/Na₂O molar ratio of the solution, was 1.46. Comparing the solution produced with SCSA/NaOH to other solutions, it presented similar better results in compressive strength tests to a solution prepared with only NaOH.

Related to other silica sources, SCSA/NaOH samples presented similar results to RHA/NaOH ones, and lower values when it was compared to the commercial sodium silicate and NaOH specimens. Microstructural analysis showed that the specimens produced from the SCSA-activating solution presented more similar results to the samples obtained from the sodium silicate/NaOH than the specimens produced by the activating solution with only NaOH.